

---

# PROBLEM SET 2

## 22.S904 Nuclear Reactor Kinetics

Due: 24 September 2012

Bryan Herman

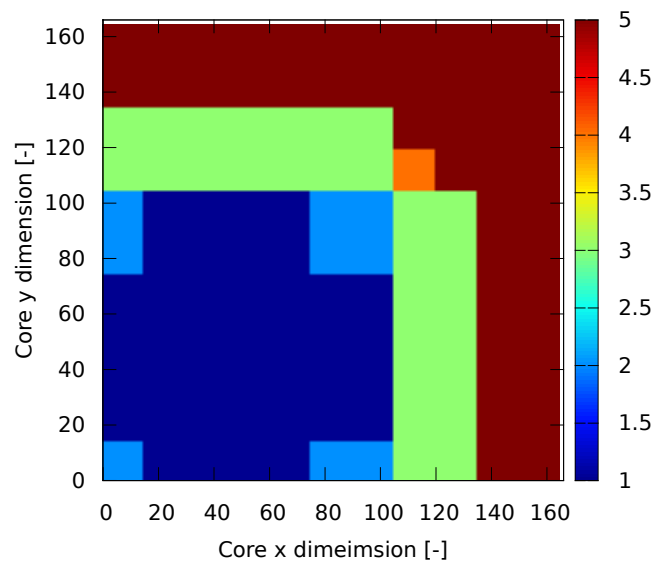
---

### Diffusion Code

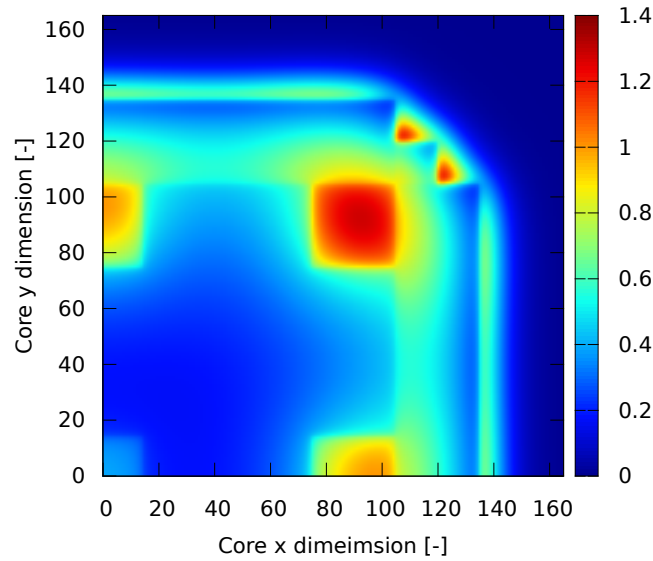
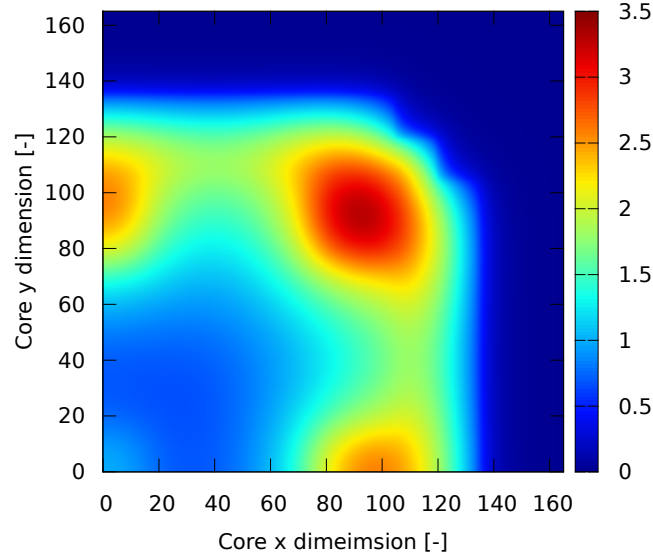
A general three-dimensional second order finite volume code was written to solve the neutron diffusion equation. **The source code can be reviewed at:**

**<http://github.com/bhermanmit/Kinetics/tree/master/HW2/src>.**

This code was verified in 2-D by running the LRA BWR benchmark. The material map how the LRA core is arranged is shown below.



Material 1 is a low enriched bundle, material 2 is medium enriched while material 3 is the highest enriched bundle. Material region 4 is exactly the same as 3 except a control rod has been ejected such that the thermal absorption cross section is lower. Finally material region 5 is the water reflector. The resulting group 1 and group 2 flux distributions are shown below.



Finally the difference in eigenvalue as compared to the benchmark reference is listed below. It shows very good agreement with the benchmark reference and gives me confidence in the diffusion solver.

My Code $k_{eff}$	Reference $k_{eff}$	$\Delta k$ (pcm)
0.99633	0.99636	3

## Part A - Difference Equations

Derive the expression for the first-order finite-difference net current at a nodal interface for the case of variable mesh spacing/material properties.

We will begin the derivation by writing expressions for the net current at a surface between two arbitrary nodes. We assume that cross sections and diffusion coefficients are constants in each cell. The surface currents are

$$\begin{aligned}\bar{J}_u^g|_{l+1/2,m,n}^- &= -D_{l,m,n}^g \left. \frac{d}{du} \bar{\phi}_u^g \right|_{l+1/2,m,n}^- \\ \bar{J}_u^g|_{l+1/2,m,n}^+ &= -D_{l+1,m,n}^g \left. \frac{d}{du} \bar{\phi}_u^g \right|_{l+1/2,m,n}^+.\end{aligned}$$

In this notation,

- $\bar{J}_u^g|_{l+1/2,m,n}^-$  is the group  $g$  surface-averaged net current at arbitrary location  $l+1/2, m, n$ , approaching the surface from the left
- $\bar{J}_u^g|_{l+1/2,m,n}^+$  is the group  $g$  surface-averaged net current at arbitrary location  $l+1/2, m, n$ , approaching the surface from the right
- $D_{l,m,n}^g$  and  $D_{l+1,m,n}^g$  are the cell-average diffusion coefficients in their respective cells
- $\left. \frac{d}{du} \bar{\phi}_u^g \right|_{l+1/2,m,n}^-$  is the gradient with respect to arbitrary direction  $u$  of the group  $g$  surface-averaged flux at location  $l+1/2, m, n$  approaching from the left
- $\left. \frac{d}{du} \bar{\phi}_u^g \right|_{l+1/2,m,n}^+$  is the gradient with respect to arbitrary direction  $u$  of the group  $g$  surface-averaged flux at location  $l+1/2, m, n$  approaching from the right

We can approximate each of these spatial derivatives by taking either a forward or back difference between the surface averaged flux and cell averaged flux, which we approximate to be the flux at the center of the cell. Therefore each equation becomes

$$\begin{aligned}\bar{J}_u^g|_{l+1/2,m,n}^- &= -D_{l,m,n}^g \frac{\bar{\phi}_u^g|_{l+1/2,m,n}^- - \bar{\phi}_{l,m,n}^g}{h_l^u/2} \\ \bar{J}_u^g|_{l+1/2,m,n}^+ &= -D_{l+1,m,n}^g \frac{\bar{\phi}_{l+1,m,n}^g - \bar{\phi}_u^g|_{l+1/2,m,n}^+}{h_{l+1}^u/2},\end{aligned}$$

where  $h_l^u$  is the width of a cell in the  $u$  direction for any cell with arbitrary index  $l$ . The first constraint place on these equations is that we have continuity of the surface flux,

$$\bar{\phi}_u^g|_{l+1/2,m,n}^- = \bar{\phi}_u^g|_{l+1/2,m,n}^+ = \bar{\phi}_{u_{l+1/2,m,n}}^g.$$

The current relations can be rewritten as

$$\bar{J}_u^g|_{l+1/2,m,n}^- = -D_{l,m,n}^g \frac{\bar{\phi}_{u_{l+1/2,m,n}}^g - \bar{\phi}_{l,m,n}^g}{h_l^u/2}$$

$$\bar{J}_u^g|_{l+1/2,m,n}^+ = -D_{l+1,m,n}^g \frac{\bar{\phi}_{l+1,m,n}^g - \bar{\phi}_{u_{l+1/2,m,n}}^g}{h_{l+1}^u/2}.$$

The next constraint is that the surface current is continuous,

$$\bar{J}_u^g|_{l+1/2,m,n}^- = \bar{J}_u^g|_{l+1/2,m,n}^+ = \bar{J}_{u_{l+1/2,m,n}}^g.$$

The current relations now become

$$\begin{aligned} \bar{J}_{u_{l+1/2,m,n}}^g &= -D_{l,m,n}^g \frac{\bar{\phi}_{u_{l+1/2,m,n}}^g - \bar{\phi}_{l,m,n}^g}{h_l^u/2} \\ \bar{J}_{u_{l+1/2,m,n}}^g &= -D_{l+1,m,n}^g \frac{\bar{\phi}_{l+1,m,n}^g - \bar{\phi}_{u_{l+1/2,m,n}}^g}{h_{l+1}^u/2}. \end{aligned}$$

Now, we are left with two equations and two unknowns. We can set both equations equal to each and solve for the surface averaged flux:

$$\begin{aligned} -D_{l,m,n}^g \frac{\bar{\phi}_{u_{l+1/2,m,n}}^g - \bar{\phi}_{l,m,n}^g}{h_l^u/2} &= -D_{l+1,m,n}^g \frac{\bar{\phi}_{l+1,m,n}^g - \bar{\phi}_{u_{l+1/2,m,n}}^g}{h_{l+1}^u/2} \\ h_{l+1}^u D_{l,m,n}^g \left( \bar{\phi}_{u_{l+1/2,m,n}}^g - \bar{\phi}_{l,m,n}^g \right) &= h_l^u D_{l+1,m,n}^g \left( \bar{\phi}_{l+1,m,n}^g - \bar{\phi}_{u_{l+1/2,m,n}}^g \right) \\ \bar{\phi}_{u_{l+1/2,m,n}}^g &= \frac{h_l^u D_{l+1,m,n}^g \bar{\phi}_{l+1,m,n}^g + h_{l+1}^u D_{l,m,n}^g \bar{\phi}_{l,m,n}^g}{h_l^u D_{l+1,m,n}^g + h_{l+1}^u D_{l,m,n}^g}. \end{aligned}$$

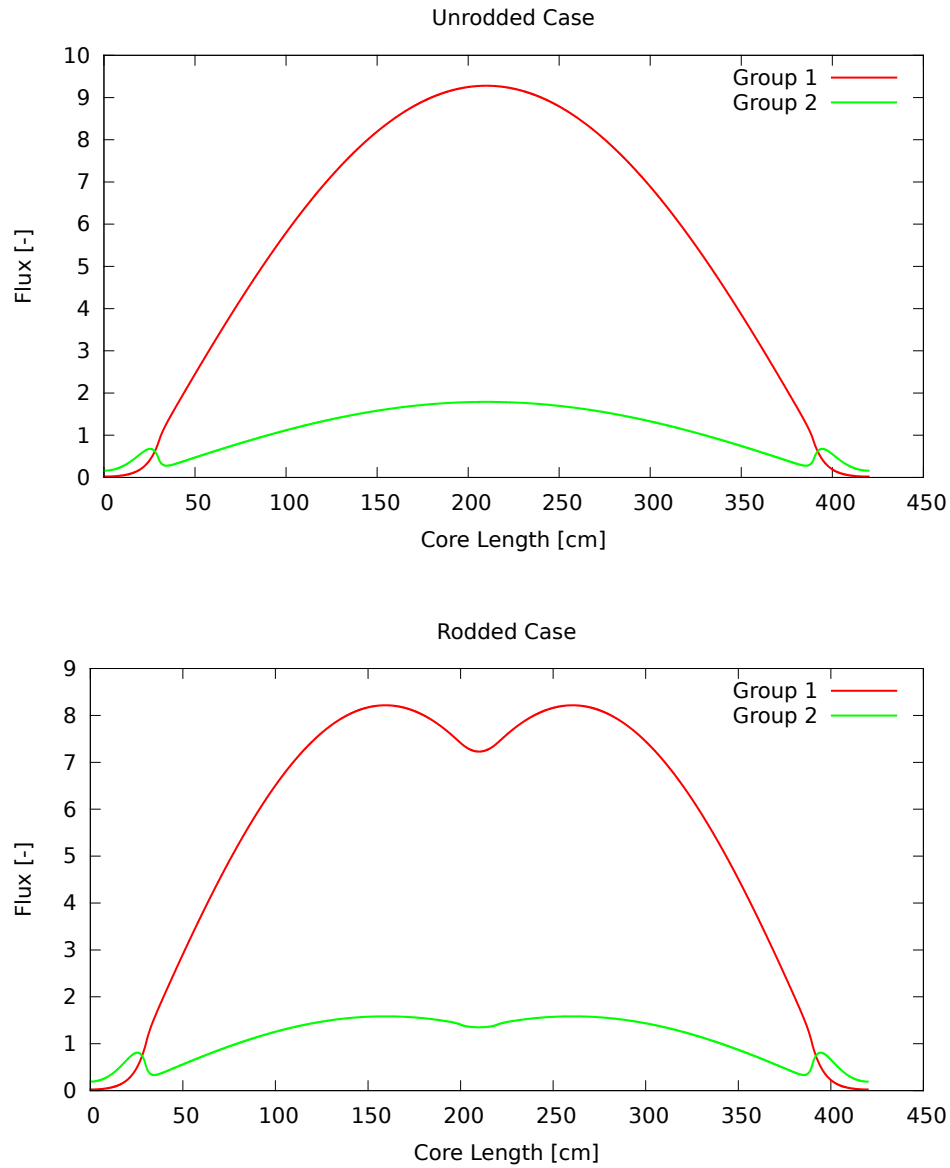
Now that we have an expression for the surface flux we can substitute into any of the current relations to get an expression for the net current. It is

$$\begin{aligned} \bar{J}_{u_{l+1/2,m,n}}^g &= -D_{l,m,n}^g \frac{\left( \frac{h_l^u D_{l+1,m,n}^g \bar{\phi}_{l+1,m,n}^g + h_{l+1}^u D_{l,m,n}^g \bar{\phi}_{l,m,n}^g}{h_l^u D_{l+1,m,n}^g + h_{l+1}^u D_{l,m,n}^g} \right) - \bar{\phi}_{l,m,n}^g}{h_l^u/2} \\ \bar{J}_{u_{l+1/2,m,n}}^g &= -\frac{2D_{l,m,n}^g}{h_l^u} \left( \frac{h_l^u D_{l+1,m,n}^g \bar{\phi}_{l+1,m,n}^g + h_{l+1}^u D_{l,m,n}^g \bar{\phi}_{l,m,n}^g}{h_l^u D_{l+1,m,n}^g + h_{l+1}^u D_{l,m,n}^g} - \frac{h_l^u D_{l+1,m,n}^g \bar{\phi}_{l,m,n}^g + h_{l+1}^u D_{l,m,n}^g \bar{\phi}_{l,m,n}^g}{h_l^u D_{l+1,m,n}^g + h_{l+1}^u D_{l,m,n}^g} \right) \\ \bar{J}_{u_{l+1/2,m,n}}^g &= -\frac{2D_{l,m,n}^g}{h_l^u} \left( \frac{h_l^u D_{l+1,m,n}^g \bar{\phi}_{l+1,m,n}^g - h_l^u D_{l+1,m,n}^g \bar{\phi}_{l,m,n}^g}{h_l^u D_{l+1,m,n}^g + h_{l+1}^u D_{l,m,n}^g} \right) \\ \boxed{\bar{J}_{u_{l+1/2,m,n}}^g} &= -\frac{2D_{l,m,n}^g D_{l+1,m,n}^g}{h_l^u D_{l+1,m,n}^g + h_{l+1}^u D_{l,m,n}^g} \left( \bar{\phi}_{l+1,m,n}^g - \bar{\phi}_{l,m,n}^g \right). \end{aligned}$$

## Part B - Spatial Convergence

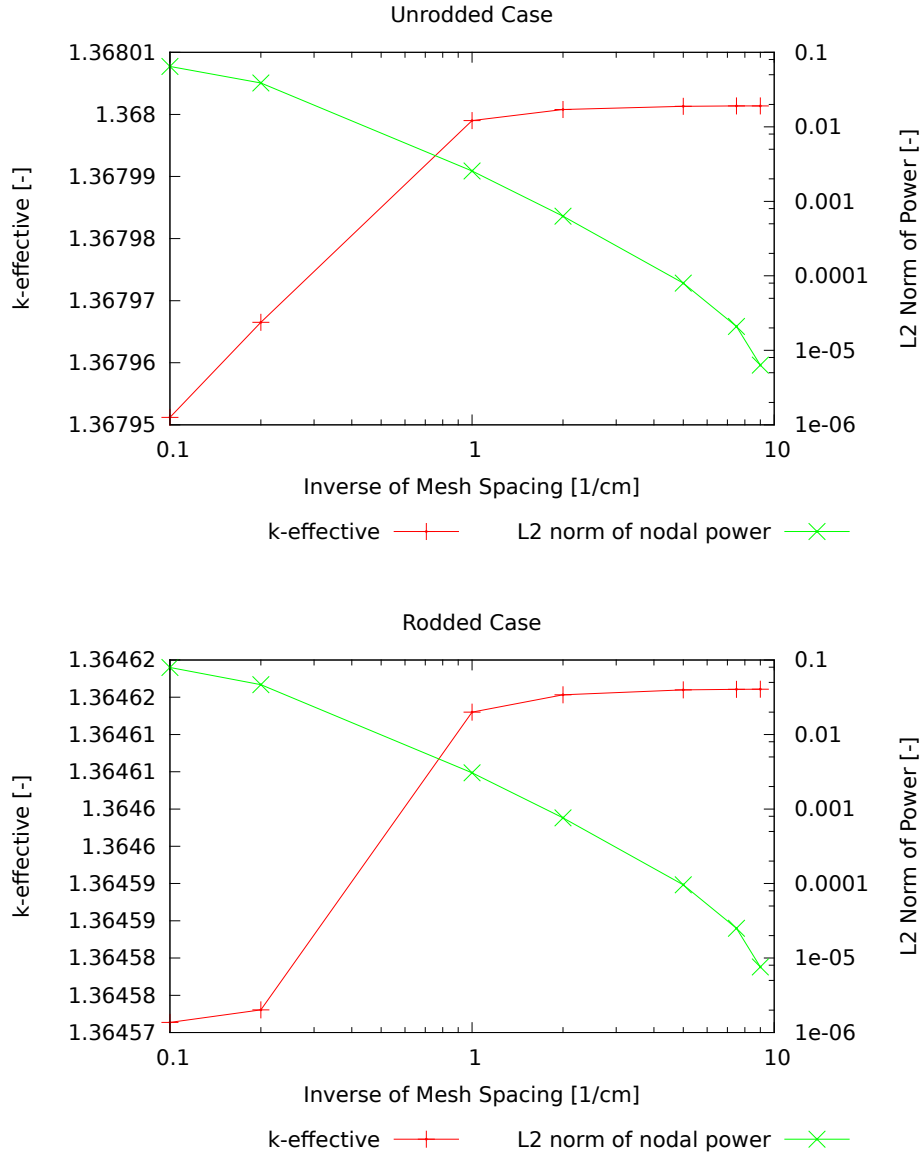
Plot the iteratively-converged eigenvalue and L2 norm of nodal power error (using 10 cm nodes) vs. mesh spacing until the L2 norm of error is converged to  $< 1e-6$  for the rodded and unrodded cores.

The reference spatial distribution chosen was 0.1 cm mesh. This was chosen due to computational requirements (the code took over an hour to run!). The eigenvalue tolerance was set at  $1e-8$ , the coarse mesh power convergence at  $1e-9$  and the G-S inner iteration tolerance was set at  $1e-10$ . The rodded and unrodded reference spatial flux distributions are shown below.



Spatial convergence plots were generated against this reference. Unfortunately, the target L2 norm of  $1e-6$  could not be met with the computer resources at hand. However, the way

this norm is defined is arbitrary. I decided to look at the L2 norm for 10 cm coarse mesh powers that were normalized to a core average of unity. Depending on this normalization, a different error can be achieved. The unrodded and rodded plots are shown below.

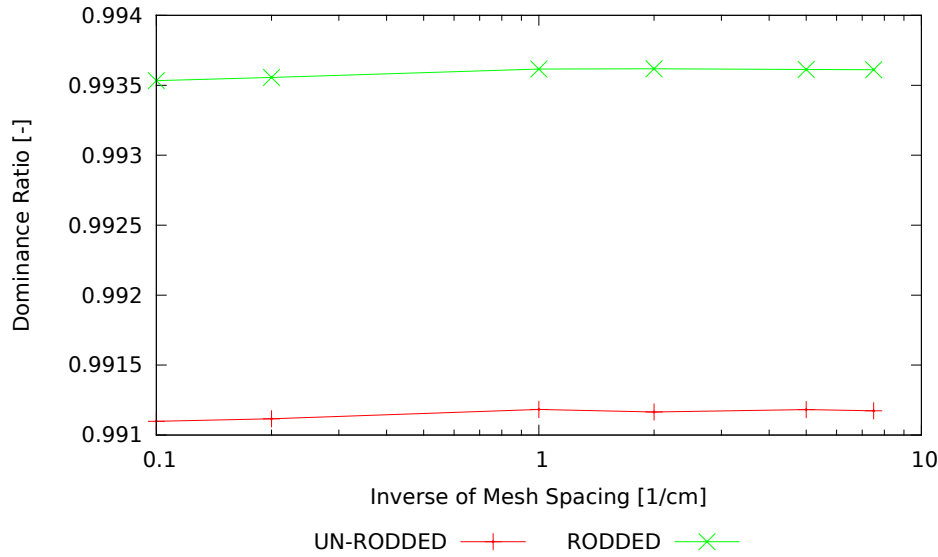


From the plots, the convergence rate is not quite second order. Also, because we get close to the reference spatial distribution a very steep slope of the convergence exists at the end. For the purposes of this homework and time, a 0.2 cm mesh will be used in subsequent parts of the homework.

## Part C - Dominance Ratio

Plot the asymptotic dominance ratio vs. mesh spacing for the rodded and unrodded cores.

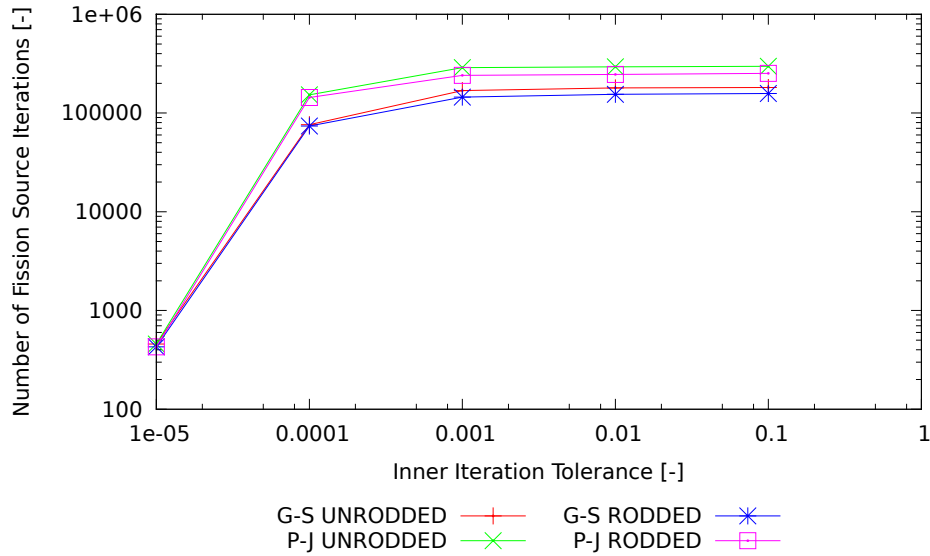
The dominance ratio is mathematically defined as the ratio of the first harmonic eigenvalue to the fundamental mode eigenvalue. Physically, the dominance ratio is impacted by geometry and material composition. Therefore, since these components remain constant when refining the mesh, we expect that the dominance ratio should not change significantly. We computed the dominance ratio as the ratio of the last L2-norm of the nodal power to the previous L2-norm of the nodal power. It agreed well with Matlab's estimate from its Arnoldi solver which gives multiple eigenvalues. **Note that we started from a random source guess to excite the first harmonic.** It was also evident that the number of fission source iterations increased. Whereas before, we started from a flat symmetric guess so the power iteration converged at the asymptotic rate of the ratio of the second harmonic to the fundamental eigenvalue. The plots shown below. From the results, the dominance ratio is not very sensitive with spatial resolution.



## Part D and Part E - Iterative Convergence of Point Jacobi and Gauss Seided

Plot the number of fission source iterations needed to achieve L2 norm of changes of nodal powers for successive fission source iterations  $< 1.e-6$  vs. flux iteration point-wise L2 norm for flux convergence criteria of  $1.e-1$ ,  $1.e-2$ ,  $1.e-3$ ,  $1.e-4$ , and  $1.e-5$  for the rodded and unrodded cores.

For this section, we are studying the effect of the tolerance on the inner iterations. In general, the higher the tolerance in the inner iterations, the more work the fission source iterations will have to do. The plot below sums up the results for the unrodded and rodded cases with point jacobi and gauss seidel.



As we can see, the lower the tolerance in the inner iterations, less fission source iterations occur. We also see that for loose inner convergence criteria point jacobi is always greater than gauss seidel. This could be due to the fact that there is only one inner iteration occurring during this time. For one iteration, gauss seidel converges faster and thus lead to fewer fission source iterations.

## Part F: Real vs. Fluxes

**What are the spatially and iteratively converged real and adjoint eigenvalues for the rodded and unrodded problems?** See plot

**What is the static rod worth in pcm?** See plot

**Plot the spatially and iteratively converged real and adjoint fluxes for the rodded and unrodded problems** See plot